REVIEW ARTICLE

Multimodal Cardiovascular Imaging of Cardiac Tumors

Ayaka Takahashi MD[1)], Hideki Otsuka MD, PhD[2)] and Masafumi Harada MD, PhD[1)]

Received: May 30, 2016/Revised manuscript received: July 20, 2016/Accepted: July 21, 2016

Abstract

Primary cardiac tumors are rare. Myxoma and sarcoma are the most common types of benign and malignant cardiac tumors, respectively. Secondary cardiac tumors, the majority of which are metastases, are more common than primary tumors. The use of an appropriate combination of cardiovascular imaging techniques is necessary for the differential diagnosis of cardiac tumors and for preoperative examinations aimed at assessing tumor mobility and the positional relationship between the tumor and the surrounding normal structures, such as valves, papillary muscle, etc. The various components of cardiac tumors, such as fibrosis, lipids, hemorrhaging, necrosis, and degenerative changes, can be identified based on their signal intensity on magnetic resonance imaging (MRI), whereas cine-MRI is useful for assessing tumor mobility. Computed tomography is the optimal modality for identifying calcification, and intravenous contrast agent injection is useful for evaluating tumor vascularity. Fluorodeoxyglucose (FDG)-positron emission tomography (PET) plays an important role in the differentiation of malignant tumors from benign ones. Malignant cells utilize more glucose than benign cells. Thus, malignant cardiac tumors exhibit more intense FDG uptake than benign tumors. PET/MRI scanners are a recently developed type of clinical imaging system that can obtain morphological, histopathological, functional, and metabolic information in a single session. To suppress physiological myocardial FDG uptake, long-term fasting; the injection of heparin; and the administration of a high fat, low carbohydrate diet can be employed before PET scans.

Herein, we review the imaging features of cardiac tumors and present clinical images of cardiac diseases that were obtained at our institution.

Keywords: Cardiac tumor, CT, FDG-PET/CT, Histopathology, MRI, PET/MRI
Ann Nucl Cardiol 2016；2（1）：61-67

Primary cardiac tumors are rare, with an autopsy incidence rate of 0.0017-0.33% (1-3). Secondary cardiac or pericardial tumors, most of which are metastases, are 20-130 times more common than primary cardiac tumors and are found in >10% of cancer patients during autopsies (1-4). Primary and secondary cardiac tumors have been classified into numerous pathological types (1). The clinical incidence of cardiac tumors varies according to when and where the study was performed. Table 1 shows the approximate frequencies of primary cardiac tumors according to several previous reports (1,5-10). About 75% of primary cardiac tumors are benign, and myxoma is the most common type of primary cardiac tumor, followed by lipoma, fibroelastoma, fibroma, and hemangioma. Rhabdomyoma and fibroma are more common in children than in adults (1,9-11). Among cavitary lesions, cardiac thrombosis, which sometimes requires surgery, is relatively common and needs to be differentiated from other cardiac tumors (12,13). About 25% of primary cardiac tumors are malignant, and sarcomatous lesions are the most frequently encountered malignant cardiac tumors (1, 5-8). However, rhabdomyosarcoma is the most common malignant cardiac tumor in children (1).

Some tumors can cause cardiac dysfunction, and the main treatment option for benign cardiac tumors is complete

doi：10.17996/ANC.02.01.61

1) Ayaka Takahashi, Masafumi Harada
Department of Radiology, Tokushima University Graduate School, Tokushima, Japan

2) Hideki Otsuka
Department of Medical Imaging / Nuclear Medicine, Tokushima University Graduate School, Kuramoto-cho 3-18-15, Tokushima city, Tokushima, Japan 770-8503
E-mail: hideki.otsuka@tokushima-u.ac.jp

Table 1 Clinical frequency of primary cardiac tumors (modified from Ref 1, 5-9)

Primary cardiac tumors	Frequency (%)
Benign	75%
Myxoma	40～90
Papillary fibroelastoma	～25
Hemangioma	5
Fibroma	<5 (20% in children)
Lipoma	<5
Rhabdomyoma	<5 (40% in children)
Paraganglioma	<5
Hamartoma	<5
Malignant	25%
Angiosarcoma	4
Rhabdomyocsarcoma	3
Other sarcoma	5
Leiomyosarcoma	
Pleomorphic liposarcoma	
Undifferentiated sarcoma	
Osteosarcoma	
Synovial sarcoma	
Malignant fibrous histiocytoma	5
Primary lymphoma	2～9

resection. Resection is also a treatment option for malignant tumors. Preoperative evaluations of the size, location, mobility, and pathology of cardiac tumors are very important. Echocardiography, computed tomography (CT), magnetic resonance imaging (MRI), and ^{18}F-fluorodeoxyglucose (FDG) positron emission tomography (PET)/CT play important roles in such evaluations (14-16). In addition, the recent development of PET/MRI scanners has led to further advances in cardiovascular imaging (17).

Herein, we review the imaging features of cardiac tumors and present images of cardiac diseases that were obtained using various techniques at our institution.

Computed tomography (CT)

CT can provide excellent anatomical and morphological information and clearly demonstrate calcification and fat components (15,18). Tumor vascularity can also be assessed using iodine contrast media. Multi-detector-row CT scans provide a wide field of view and a high spatial resolution, can be performed with and without electrocardiography (ECG)-gated protocols, and do not take long. Three-dimensional or multiplanar reconstruction images can also be obtained. Tumor movement and the locations of cardiac valves and the myocardium can be evaluated on ECG-gated cine-CT. In addition, advances are being made in low radiation dose and high spatial resolution techniques (19).

Magnetic resonance imaging (MRI)

MRI is superior to tissue characterization using numerous scan parameters. Signal intensity can be used as an indicator of the histopathological state of the target tissue. Adipose tissue exhibits high intensity on both T1-weighted imaging (WI) and T2WI, and signal loss is evident in such regions on fat-suppressed sequences. On T2WI, fibrotic tissue displays low intensity, and edema demonstrates high intensity. Hemorrhaging or degeneration can show various signal intensities. Many malignant tumors display high intensity on diffusion-weighted imaging, depending on their tumor cell density or the degree of diffusion impairment. Cine-MRI and contrast-enhanced MRI are also useful for tumor evaluations. However, MRI is of limited use in cases involving patients with claustrophobia or implanted metallic devices, such as non-MRI-conditional cardiac pacemakers (who cannot undergo MRI). On the other hand, MRI-conditional cardiac devices have recently been developed and are available in the clinical setting (14,15,20-22).

Fluorodeoxyglucose-positron emission tomography/CT (FDG-PET/CT)

FDG is a glucose analog that has been labeled with the fluorine-18 positron and accumulates in some tumors and active inflammatory lesions, such as cardiac sarcoidosis and vasculitis (23,24). FDG-PET/CT can provide both morphological and metabolic images of the whole body in a single session, and is very useful for tumor staging, detecting recurrence, predicting prognosis, and therapeutic monitoring (25-27). Both primary and secondary cardiac tumors can be evaluated using FDG-PET/CT. In cases of cardiac metastasis, FDG-PET/CT can detect both the primary lesions, such as lung cancer, esophageal cancer, etc., and the cardiac metastasis. In cardiac lymphoma, FDG-PET/CT is useful for staging and can clarify whether a cardiac lesion is a primary lesion or represents an extra-nodal form of systemic lymphoma. Malignant tumors utilize much more glucose than benign ones. Thus, strong FDG uptake is seen in malignant tumors, whereas benign tumors demonstrate no to faint FDG uptake. The extent of FDG uptake reflects the degree of histopathological malignancy, and evaluations of FDG uptake are useful for differentiating between benign and malignant lesions (28, 29). The standardized uptake value (SUV) is a quantitative parameter that indicates the degree of FDG uptake in a lesion corrected for body weight and the injected FDG dose, assuming that the FDG is evenly distributed throughout the body (30). Malignant cardiac tumors display high SUV, and benign cardiac tumors exhibit lower SUV than malignant

Table 2 Summary of the SUV_{max} of cardiac tumors

		Malignant				Benign		
		Range	Mean	Median		Range	Mean	Median
Shao (16), n; 23	n; 13	4.1－21.2	not available	6.5	n; 10	0.5－7.4	not available	1.5
Rahbar (30) n; 24	n; 17	3.8－16.7	9.5	8.7	n; 7	1.6－4	2.8	2.7
Nensa (36) n; 20	n; 7	5.2－21.3	13.2	13.6	n; 13	1－5.2	2.2	2.0
Kikuchi (31) n; 17	n; 14	3.2－22.6	14	14.6	n; 3	0.9－6.8	3.4	2.6

		Malignant lymphoma		Myxoma
		Range		Range
Kikuchi (31)	n; 3	22.2－29	Rahbar (30) n; 3	1.6－4
Rahbar (30)	n; 2	13.7, 16.7		
Nensa (36)	n; 1	7.6		Thrombus
				Range
		Metastases	Nensa (36) n; 3	1－2
		Range		
Rahbar (30)	n; 6	3.8－15.5		
Nensa (36)	n; 3	5.2－20.7		
Kikuchi (31)	n; 7	3.2－15.3		

Malignant tumors exhibit greater SUV_{max} than benign tumors. n: number of cases.
SUV_{max} in Ref.36 was calculated with MR-based attenuation correction.

ones. However, cardiac tumors are rare, and there have been few studies about the FDG-PET findings of cardiac tumors involving a large number of patients. Although there is no clear SUV_{max} cut-off value for differentiating between malignant and benign cardiac tumors, malignant tumors have greater SUV_{max} values than benign tumors. Table 2 shows the SUV_{max} values of cardiac lesions reported in the literature. It is proposed that the optimum cut-off SUV_{max} value for differentiating between malignant and benign cardiac tumors is 3.5-4.0 (16,30). In particular, diffuse large B-cell lymphoma (DLBCL) tends to exhibit greater SUV_{max} values than other malignant cardiac tumors (31). Regarding the detection of cardiac tumors on FDG-PET, physiological FDG accumulation in the myocardium can sometimes be problematic. Physiological cardiac FDG uptake exhibits four different patterns (none, diffuse, focal, and focal on diffuse) and can mask lesions (32). Long-term fasting and low-carbohydrate diet consumption are used to reduce physiological FDG accumulation in the myocardium (33).

FDG-PET/MRI

PET/MRI scanners are a newly developed type of clinical imaging system (34). They benefit from the advantages of both PET, which exhibits superior performance during metabolic imaging, and MRI, which demonstrates superior performance during morphological and tissue characterization (17, 34). Regarding the differences between PET/CT and PET/MRI, PET/MRI reduces the patient's radiation exposure, but takes longer to perform, as MRI are obtained with various MRI sequences instead of CT images. PET data can be subjected to attenuation correction via segmented attenuation mapping, in which the target tissue is classified into four types (background, lung tissue, fat, and soft tissue) using the Dixon MRI sequence (35). In addition, gadolinium-enhanced studies are useful for evaluating tumor vascularity, and ECG-gated sequences, breath-holding sequences, and late gadolinium enhancement (LGE) are also appropriate in certain cases (36). Nensa reported the FDG-PET/MRI findings of 20 patients with cardiac tumors (36). To reduce physiological FDG uptake in the myocardium, the patients were told to consume a high-fat, low carbohydrate diet and were injected with heparin before the scan. SUV were calculated with MRI-based attenuation correction (35). An SUV_{max} cut-off value of ≥5.2 was found to exhibit 100% sensitivity and 92% specificity for differentiating malignant cardiac lesions from benign ones on FDG-PET. During the MRI scans, tumor size; the presence/absence of pericardial effusion; cine morphology; and hyperintensity were evaluated on T1WI, T2WI, and contrast-enhanced scans. The examination of such MRI features resulted in 100% sensitivity and 92% specificity for differentiating malignant lesions from benign ones. Similarly, the combined use of a cut-off SUV_{max} of 5. 2 and the abovementioned MRI features exhibited 100% sensitivity and 100% specificity for differentiating malignant cardiac lesions from benign ones.

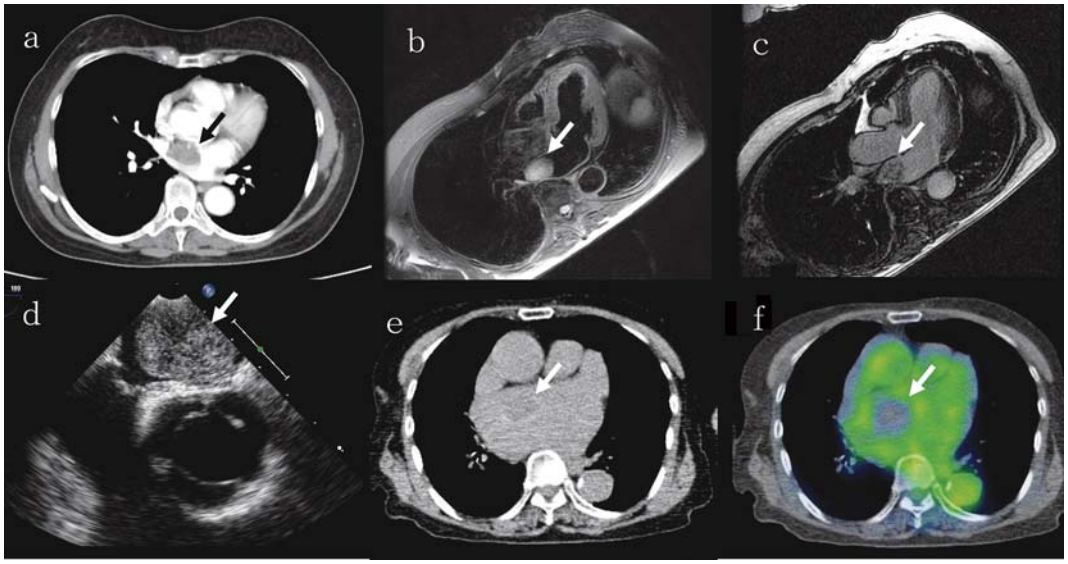

Fig. 1 A myxoma (a-d) and an intracavitary thrombus (reference case) (e, f)
a: Contrast-enhanced (CE) CT, b: MRI T2WI, c: MRI CE-T1WI, d: Echocardiography, e: non-CE CT, f: FDG-PET/CT
The myxoma was located in the left atrium and was attached to the atrial septum. The base of the tumor appeared to be located in the atrial septum. On MRI, the myxoma exhibited low intensity on T1WI, high intensity on T2WI, and heterogeneous contrast enhancement. Echocardiography showed a heterogeneous echoic mass.
e, f: CT and FDG-PET/CT image of a thrombus in the left atrium
The thrombus displayed low density on CT, and no FDG uptake was seen within the thrombus.

Image presentation

Benign tumors

Myxoma

Myxoma accounts for 25-50% of primary cardiac tumors and is the most common primary cardiac tumor affecting adults. It predominantly arises in females in their 30s to 40s. Myxomas occur in the left and right atria in 60-75% and approximately 20% of cases, respectively (18, 37). Most myxomas adhere to the atrial septum, and their mobility can be assessed using echocardiography or cine-MRI. Myxomas can be spherical or ovoid shaped; have smooth margins; consist of various components, such as myxoid and fibrous tissue and calcifications; and can exhibit hemorrhaging. Myxomas display low to iso-density on non-contrast-enhanced CT (14, 18). Calcification is more common in right atrial masses and is clearly shown on CT. On MRI, myxomas typically display low intensity on T1WI and high intensity on T2WI; however, they sometimes exhibit heterogeneous signal intensity due to mucoid degeneration or hemorrhaging (21). Faint contrast enhancement is seen in the arterial phase, and mild contrast enhancement is observed in the delayed phase (Fig. 1a-c). On FDG-PET/CT, myxomas display faint to mild FDG uptake. It is important to differentiate myxomas from intracardiac thrombi. Thrombi exhibit high intensity on MRI T1WI, but do not display contrast enhancement on CT or MRI or FDG avidity on FDG-PET/CT (13) (Fig. 1e, f).

Lipoma

Lipoma is the second most common primary benign cardiac tumor, accounting for 8-12% of such lesions (20). Lipomas can occur at any time of life and predominantly arise in the atrial septum, right atrium, and left ventricle. About 50% of lipomas arise from the mid-myocardial layer to epicedium, and the other half arise from the subendocardium (18). Lipomas are composed of mature adipose tissue and do not display calcification, hemorrhaging, or solid components. Both CT and MRI are useful for detecting the characteristic features of lipoma. On CT, lipomas exhibit homogeneous low density (fat density, CT value: less than -50 Hounsfield units). On MRI, lipomas demonstrate the same signal intensity as fat on both T1WI and T2WI, and their signal intensity decreases on fat-suppression sequences. In cases in which the tumor exhibits a solid component or contrast enhancement, liposarcomas and teratomas should be included in the differential diagnoses.

Fibroma

Fibromas, which consist of fibroblasts, commonly arise as primary cardiac tumors in children. Cardiac fibroma can cause arrhythmia or sudden cardiac death. The macroscopic features of cardiac fibroma include a well-defined mass that is mainly located in the interventricular septum, and central calcification is also often seen. Central calcification in a solitary mass can be used to differentiate cardiac fibromas from rhabdomyomas. CT is superior to MRI for detecting calcification (18). Cardiac

fibromas exhibit iso- or low intensity on T1WI and low intensity on T2WI, reflecting the fibrous tissue they contain. The contrast enhancement patterns of cardiac fibromas vary. LGE is seen in the delayed phase due to the presence of fibroblasts interspersed among a large amount of collagen, and this has been suggested to be another characteristic finding of cardiac fibromas (38). Masuda et al. reported that the abovementioned signal intensity pattern and the presence of LGE on MRI are very useful for differentiating an intensely FDG-avid cardiac fibroma from other malignant tumors (39).

Malignant tumors

Malignant lymphoma

About 16-28% of malignant lymphoma patients exhibit cardiac involvement (40), but primary cardiac lymphomas are rare, accounting for 0.5% of all lymphomas and about 1.3-2% of all cardiac tumors. More than 80% of primary cardiac lymphomas are DLBCL. Such tumors often develop in immunocompromised patients (41). As for their radiological features, primary cardiac lymphomas occur on the right side of the heart more frequently than other cardiac tumors. In cases of primary cardiac lymphoma, the coronary artery usually remains patent, and coronary blood flow passes through the mass in an unimpaired manner. Cardiac lymphomas are usually solid homogeneous masses, and a large amount of pericardial effusion is seen in some cases (31). Chemotherapy is effective against cardiac lymphoma, and pre-treatment clinical imaging plays a very important role in avoiding unnecessary invasive procedures. On MRI, such tumors display isointensity on T1WI and iso- to low intensity and heterogeneous contrast enhancement on T2WI. Malignant lymphoma is a systemic disease, and FDG-PET/CT is very useful for tumor staging, prognostic prediction, evaluating the early response to chemotherapy, and detecting relapses (42). Lymphomas commonly demonstrate strong FDG uptake. In the present study, the mean SUVmax of DLBCL was 25.9, which was significantly higher than those of other cardiac tumors (the mean SUV_{max} of malignant cardiac tumors was 10.5, and that of benign cardiac tumors was 3.4) (Fig.2) (31).

Metastatic cardiac tumors

Metastatic cardiac tumors occur significantly more frequently than primary ones. Such tumors are found in 10-12% in autopsy studies of patients with malignant neoplasms (43, 44). Cardiac metastases are most commonly derived from primary malignant tumors of the lungs (35-40%), followed by primary malignant tumors of the breast (7.3-12%) and hematological malignancies (10-21%) (18,43). Such metastases most frequently arise in the pericardium (64-69%) and myocardium (29-32%). Endocardial or intracavitary metastatic tumors are rare (3-5%) (43). In the case of pericardial metastases, irregular thickening of the pericardium and pericardial effusion are often seen. After myocardial invasion, nodular masses develop in the myocardium. On MRI, such masses typically exhibit low intensity on T1WI and high intensity on T2WI. However, these findings are non-specific and are not useful for distinguishing metastatic cardiac tumors from other cardiac tumors. As mentioned previously, strong FDG uptake on PET/CT might be useful for diagnosing metastatic cardiac tumors, and PET/CT can also be employed for whole-body scans aimed at detecting residual lesions.

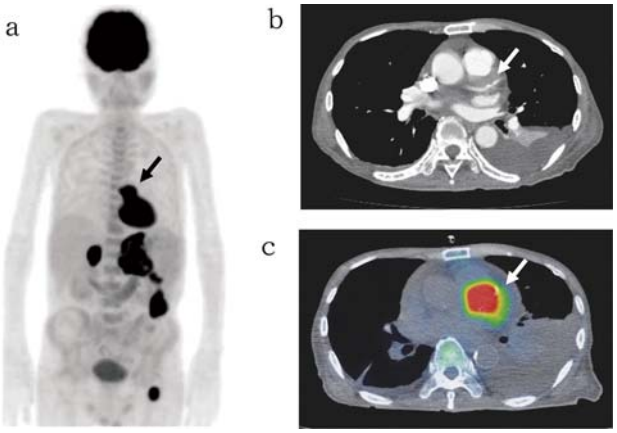

Fig. 2 a-c: Malignant lymphoma
a: Whole-body FDG-PET. FDG-PET detected systemic lesions (in the pericardium, bilateral adrenal glands, abdominal cavity, and left femur). b: CE CT of a malignant lymphoma arising from the pericardium. The left coronary artery passed through the tumor (arrow). c: FDG-PET/CT. The pericardial lesion showed very strong FDG uptake (SUV_{max}: 28.2).

Conclusions

The use of an appropriate combination of cardiovascular imaging techniques is important for the differential diagnosis of cardiac tumors and for preoperative evaluations aimed at clarifying the mobility of cardiac tumors and the positional relationship between such tumors and the surrounding normal structures, such as cardiac valves and papillary muscle.

Acknowledgments

The authors acknowledge Mr. Yamato Kunikane RT and all of the nuclear medicine staff for their assistance in the preparation of the manuscript

Sources of funding

None

Conflicts of interest

None of the authors has any conflicts of interest to declare.

Reprint requests and correspondence:
Hideki Otsuka, MD, PhD
Department of Medical Imaging / Nuclear Medicine, Tokushima University Graduate School, Kuramoto-cho 3-18-15, Tokushima city, Tokushima, Japan 770-8503
E-mail: hideki.otsuka@tokushima-u.ac.jp

References

1. Amano J, Nakayama J, Yoshimura Y, et al. Clinical classification of cardiovascular tumors and tumor-like lesions, and its incidences. Gen Thorac Cardiovasc Surg 2013; 61: 435-47.
2. Butany J, Leong SW, Carmichael K, et al. A 30-year analysis of cardiac neoplasms at autopsy. Can J Cardiol 2005; 21: 675-80.
3. Lam KY, Dickens P, Chan AC. Tumors of the heart. A 20-year experience with a review of 12,485 consecutive autopsies. Arch Pathol Lab Med 1993; 117: 1027-31.
4. Klatt EC, Heitz DR. Cardiac metastases. Cancer 1990; 65: 1456-9.
5. Yin L, He D, Shen H, et al. Surgical treatment of cardiac tumors: a 5-year experience from a single cardiac center. J Thorac Dis 2016; 8: 911-9.
6. Anvari MS, Naderan M, Eslami Shahr Babaki A, et al. Clinicopathologic review of non-myxoma cardiac tumors: a 10-year single-center experience. Cardiology 2014; 129: 199-202.
7. Elbardissi AW, Dearani JA, Daly RC, et al. Survival after resection of primary cardiac tumors: a 48-year experience. Circulation 2008; 118: S7-15.
8. Centofanti P, Di Rosa E, Deorsola L, et al. Primary cardiac tumors: early and late results of surgical treatment in 91 patients. Ann Thorac Surg 1999; 68: 1236-41.
9. Linnemeier L, Benneyworth BD, Turrentine M, et al. Pediatric cardiac tumors: a 45-year, single-institution review. World J Pediatr Congenit Heart Surg 2015; 6: 215-9.
10. Delmo Walter EM, Javier MF, Sander F, et al. Primary Cardiac Tumors in Infants and Children: Surgical Strategy and Long-Term Outcome. Ann Thorac Surg 2016 Jun 23. [Epub ahead of print]
11. Tao TY, Yahyavi-Firouz-Abadi N, Singh GK, et al. Pediatric cardiac tumors: clinical and imaging features. Radiographics 2014; 34: 1031-46.
12. Srichai MB, Junor C, Rodriguez LL, et al. Clinical, imaging, and pathological characteristics of left ventricular thrombus: a comparison of contrast-enhanced magnetic resonance imaging, transthoracic echocardiography, and transesophageal echocardiography with surgical or pathological validation. Am Heart J 2006; 152: 75-84.
13. Rinuncini M, Zuin M, Scaranello F, et al. Differentiation of cardiac thrombus from cardiac tumor combining cardiac MRI and ^{18}F-FDG-PET/CT Imaging. Int J Cardiol 2016; 212: 94-6.
14. Grebenc ML, Rosado de Christenson ML, Burke AP, et al. Primary cardiac and pericardial neoplasms: radiologic-pathologic correlation. Radiographics 2000; 20: 1073-103.
15. Hoey ET, Mankad K, Puppala S, et al. MRI and CT appearances of cardiac tumours in adults. Clin Radiol 2009; 64: 1214-30.
16. Shao D, Wang SX, Liang CH, et al. Differentiation of malignant from benign heart and pericardial lesions using positron emission tomography and computed tomography. J Nucl Cardiol 2011; 18: 668-77.
17. Ratib O, Nkoulou R. Potential Applications of PET/MR Imaging in Cardiology. J Nucl Med 2014; 55: 40S-6S.
18. Kassop D, Donovan MS, Cheezum MK, et al. Cardiac Masses on Cardiac CT: A Review. Curr Cardiovasc Imaging Rep 2014 7: 9281.
19. den Harder AM, Willemink MJ, de Jong PA, et al. New horizons in cardiac CT. Clin Radiol 2016; 71: 758-67.
20. O'Donnell DH, Abbara S, Chaithiraphan V, et al. Cardiac tumors: Optimal Cardiac MR sequences and spectrum of imaging appearances. AJR Am J Roentgenol 2009; 193: 377-87.
21. Sparrow PJ, Kurian JB, Jones TR, et al. MR imaging of cardiac tumors. Radiographics 2005; 25: 1255-76.
22. Zhu D, Yin S, Cheng W, et al. Cardiac MRI-based multi-modality imaging in clinical decision-making: Preliminary assessment of a management algorithm for patients with suspected cardiac mass. Int J Cardiol 2016; 203: 474-81.
23. Yoshinaga K, Manabe O, Ohira H, et al. Focus issue on cardiac sarcoidosis from international congress of nuclear cardiology and cardiac CT (ICNC 12) symposium: improving the detectability of cardiac sarcoidosis -practical aspects of 18F-fluorodeoxyglucose positron emission tomography imaging for diagnosis of cardiac sarcoidosis-. Ann Nucl Cardiol 2015; 1 (1): 87-94.
24. Otsuka H, Morita N, Yamashita K, et al. FDG-PET/CT for diagnosis and follow-up of vasculitis. J Med Invest 2007; 54: 345-9.
25. Yang Z, Xu W, Ma Y, et al. ^{18}F-FDG PET/CT can correct the clinical stages and predict pathological parameters before operation in cervical cancer. Eur J Radiol 2016; 85: 877-84.
26. Otsuka H, Graham MM, Kogame M, et al. The impact of FDG-PET in the management of patients with salivary gland malignancy. Ann Nucl Med 2005; 19: 691-4.
27. Wahl RL, Jacene H, Kasamon Y, et al. From RECIST to PERCIST: evolving considerations for PET response criteria in solid tumors. J Nucl Med 2009; 50: 122S-50S.
28. Otomi Y, Otsuka H, Terazawa K, et al. Comparing the performance of visual estimation and standard uptake value of F-18 fluorodeoxyglucose positron emission tomography/computed tomography for detecting malignancy in pancreatic tumors other than invasive ductal carcinoma. J Med Invest 2014; 61: 171-9.
29. Nose H, Otsuka H, Otomi Y, et al. Correlations between F-18 FDG PET/CT and pathological findings in soft tissue lesions. J Med Invest 2013; 60: 184-90.
30. Rahbar K, Seifarth H, Schäfers M, et al. Differentiation of malignant and benign cardiac tumors using ^{18}F-FDG PET/CT. J Nucl Med 2012; 53: 856-63.
31. Kikuchi Y, Oyama-Manabe N, Manabe O, et al. Imaging characteristics of cardiac dominant diffuse large B-cell lymphoma demonstrated with MDCT and PET/CT. Eur J Nucl Med Mol Imaging 2013; 40: 1337-44.
32. Nose H, Otsuka H, Otomi Y, et al. The physiological uptake

pattern of ^{18}F-FDG in the left ventricular myocardium of patients without heart disease. J Med Invest 2014; 61: 53-8.
33. Manabe O, Yoshinaga K, Ohira H, et al. The effects of 18-h fasting with low-carbohydrate diet preparation on suppressed physiological myocardial ^{18}F-fluorodeoxyglucose (FDG) uptake and possible minimal effects of unfractionated heparin use in patients with suspected cardiac involvement sarcoidosis. J Nucl Cardiol 2016; 23: 244-52.
34. Jadvar H, Colletti PM. Competitive advantage of PET/MRI. Eur J Radiol 2014; 83: 84-94.
35. Martinez-Möller A, Souvatzoglou M, Delso G, et al. Tissue classification as a potential approach for attenuation correction in whole-body PET/MRI: evaluation with PET/CT data. J Nucl Med 2009; 50: 520-6.
36. Nensa F, Tezgah E, Poeppel TD, et al. Integrated ^{18}F-FDG PET/MR imaging in the assessment of cardiac masses: a pilot study. J Nucl Med 2015; 56: 255-60.
37. Grebenc ML, Rosado-de-Christenson ML, Green CE, et al. Cardiac myxoma: imaging features in 83 patients. Radiographics 2002; 22: 673-89.
38. Gravina M, Casavecchia G, Totaro A, et al. Left ventricular fibroma: what cardiac magnetic resonance imaging may add? Int J Cardiol 2014; 176: e63-5.
39. Masuda A, Manabe O, Oyama-Manabe N, et al. Cardiac fibroma with high ^{18}F-FDG uptake mimicking malignant tumor. J Nucl Cardiol 2015 Dec 16. [Epub ahead of print]
40. Tai CJ, Wang WS, Chung MT, et al. Complete atrioventricular block as a major clinical presentation of the primary cardiac lymphoma: a case report. Jpn J Clin Oncol 2001; 31: 217-20.
41. Hsueh SC, Chung MT, Fang R, et al. Primary cardiac lymphoma. J Chin Med Assoc 2006; 69: 169-74.
42. Seam P, Juweid ME, Cheson BD. The role of FDG-PET scans in patients with lymphoma. Blood 2007; 110: 3507-16.
43. Goldberg AD, Blankstein R, Padera RF. Tumors metastatic to the heart. Circulation 2013; 128: 1790-94.
44. Chiles C, Woodard PK, Gutierrez FR, et al. Metastatic involvement of the heart and pericardium: CT and MR imaging. Radiographics 2001; 21: 439-49.